Highlights on Spanish Astrophysics X, Proceedings of the XIII Scientific Meeting of the Spanish Astronomical Society held on July 16 – 20, 2018, in Salamanca, Spain. B. Montesinos, A. Asensio Ramos, F. Buitrago, R. Schödel, E. Villaver, S. Pérez-Hoyos, I. Ordóñez-Etxeberria (eds.), 2019

The stellar cusp around the Milky Way's central black hole.

E. Gallego-Cano[1], R. Schödel[1], B. Shahzamanian[1], H. Dong[1], F. Nogueras-Lara[1], and A. T. Gallego-Calvente[1]

[1] Instituto de Astrofísica de Andalucía (CSIC), Glorieta de la Astronomía s/n, 18008 Granada, Spain

Abstract

The formation of a stellar cusp in a dense cluster around a massive black hole is a fundamental prediction of theoretical stellar dynamic, that has not been confirmed satisfactorily by observations so far. We address its study in the most suited laboratory: the inner parsecs at the Galactic centre. With improved methodologies, we find strong evidence of the existence of the stellar cusp around the Milky Ways's supermassive black hole, reaching finally an agreement between the theory and observation. The result is not only relevant for the Galactic centre but it has implications on other galactic nuclei and future observations, such as the frequency of observations of Extreme-Mass Ratio Inspirals with gravitational wave detectors.

1 Introduction

The majority of nearby galaxies have at their centres nuclear stellar clusters (NSCs), the densest and most massive stellar clusters (SCs) in the universe (see review by [28]). They are composed of multiple stellar populations, presenting a complex (even recent) star formation (SF) history, and they can coexist with massive black holes (BH). The study of NSCs can help us to make progress in many astrophysical fields (for example SF under extreme conditions) and study stellar dynamics, such as the formation of stellar cusps. Theoretical stellar dynamics predicts firmly the formation of a stellar cusp around a massive BH in a dense and dynamically relaxed SC (e.g., [24, 3, 15, 22]). They reach the same conclusion, by using analytical, Monte Carlo and N-body simulation: the stellar number density is described by a power law of the form $\rho \sim r^{-\gamma}$, where ρ is the stellar density and r is the distance from the black hole. For an SC composed of a single-mass stellar population, the cusp is developing with $\gamma = 1.75$ inside the radius of influence of the central BH. In general, if the SC consists of a range of stellar masses, we would expect a value of gamma between $1.5 - 2$, greater values for larger stellar masses.

Nevertheless, there are not observational confirmations supporting unambiguously the existence of stellar cusps up to now. Due to the great distance of the extragalactic systems, we only can study the light density averaged of hundreds to thousands (even millions) of stars, that in general are dominated by the brightest and youngest stars and therefore, not dynamically relaxed.

The Galactic centre (GC) is an ideal case for testing the existence of a stellar cusp. It is the closest nucleus of a galaxy, located at only ~ 8.12 kpc from Earth [21] and it has a $4 \times 10^6\,\mathrm{M}_\odot$ [6, 20, 21] massive BH, Sagittarius A* (Sgr A*), surrounded by a $\sim 2.5 \times 10^7\,\mathrm{M}_\odot$ NSC [31, 32, 13, 8, 14]. We can actually resolve the stars observationally on scales of about 2 milli-parsecs inside the radius of influence of the BH (~ 3 pc [1, 17, 33]). However, we can not find strong evidence for the existence (or not) of a stellar cusp at the GC so far. Many previous works have studied the surface of old stars. The first studies found a cusp-like structure [19, 30], but the successive ones, after removing properly young stars from the sample, determined that the distribution of stars around Sgr A* shows a core-like profile, resulting in the so-called *missing cusp* problem [4, 7, 11, 30]. Many theoretical papers have tried to explain this lack of cusp, mainly in two different research lines. On the one hand, some of them claim that the distribution that we observe is representative for the entire old population and there is no cusp, perhaps because the relaxation time is very long ($>> 10$ Gyr) [25] or because the cusp has been already destroyed [26]. On the other hand, other studies suggest that the distribution we observe is only representative for bright stars, and there is a hidden cusp. They explain the deficit of giants around Sgr A* by the destruction of their envelopes rendering them to invisible for observations, due to stellar collisions, that do not be able to fully explain the observed distribution [9], or fragmenting stellar discs, that [2] can.

The most important difficulty that we have to overcome to study this fundamental problem of theoretical stellar dynamics is the stellar classification. We have to select suited tracer populations, old enough to be dynamically relaxed. Due to the extreme interstellar extinction toward the GC and source crowding, observations studies are very challenging. The spectroscopic identification of stars is limited to brightest giants and massive, young stars ($\mathrm{K} \leq 16$). Moreover, the SF history of the NSC is complex: we find stellar population made up of multiple generations of stars: old (> 1 Gyr) population of stars, but also a young generation of stars (< 100 Myr). In order to study the cusp, we have to focus on stars with ages greater than the relaxation time at the GC (a few Gyr [1]). Only red clump (RC) stars fulfil that condition up to now and dominate the measurements. Moreover, the NSC is not isolated, so that when we measure stars number density and diffuse flux toward the GC, we find several superposed components: Galactic disc (GD), Galactic bulge (GB), nuclear stellar disc (NSD) and NSC. Therefore, our knowledge about the stellar population is limited to the brightest few percents of stars, either few million-year old hot post main sequence (MS) giants and MS O/B stars, or giants on the RC. In fact, the only study that analyzed fainter stars found a cusp within $5''/0.2$pc of Sgr,A* [34]. We present the latest works addressing the distribution of stars around Sgr A* with improved methodologies to reach the faintest stars studied so far and test other possibly tracer populations.

2 Data and methodology

In order to study the distribution of stars around Sgr A*, we use data obtained with NACO instrument at the ESO/Very Large Telescope (VLT) and we focus on two different methods to analyze three different stellar populations.

2.1 Star counts

We use S27 camera data with $0.027''$ pixel scale in H-band from 9 May/2010 and in K_s-band from 9 August/11-12 September 2012. All the data were acquired with similar four-point dither pattern centred on Sgr A*, that covers a field of view (FOV) of about $40'' \times 40''$ (deep mosaic in the left panel in Figure 1). Moreover, we use K_s-band data from 11 May 2012 in order to study larger distances. They cover a wider mosaic of about $1.5' \times 1.5'$ with a 4×4 dither pattern, centred on Sgr A*. The data are summarised in Table 1 from [17]. The standard data reduction (sky subtraction, bad pixel removal and flat fielding) was improved by rebbining the images a factor of two, via a quadratic interpolation, and removing of systematic horizontal noise from detector electronics. The final images were aligned, staked and combined in a simple mean. We also included the wider mosaic with a larger FOV, obtained the Figure 6 in [17]. We implemented the source detection, astrometry, and photometry with the point spread function (PSF) fitting program *StarFinder* [10]. We took into account the variability of the PSF across the FOV, and we divided the FOV into small sub-fields ($10'' \times 10''$), smaller than the isoplanatic angle. We enhanced the PSF extraction by considering the halo of the brightest star in the field GCIRS7 joined with the local PSF for each concrete sub-field. Moreover, we considered explicitly the systematic errors derived by the choice of the *StarFinder* parameters, by considering different sets of values to analyze the images. The methodology is described in detail in [17].

2.2 Diffuse light

We use the same data described in the previous Section but we add K_s-band VLT/NACO S13 camera data from 4 May/12 June/13 August 2011, 4 May/9 August/12 September 2012, and 29 March/14 May 2013. We also add the intermediate band (IB) filter imaging data at 2.27μm (details in Table 1 of [7]). We proceeded in the same way that we explained before, but we took care especially of the subtraction of stars close to the brightest stars (GCIRS7, IRS 16, IRS 1, IRS 33 and IRS 13) concentrated in the inner 0.5 pc, which is a critical step in the analysis of the diffuse light. Another crucial point is the correction of the so-called mini-spiral (see e.g.[18]). Therefore, we subtracted from our images the calibrated HST/NICMOS 3 image of the gas emission at 1.87μm from [12] (see left panel in Figure 2 of [33]). The details of the analysis are described meticulously in [33]. Figure 1 shows the different results obtained along with all the procedure. The middle and right panels show the same image with all detected stars subtracted by using a simple, constant PSF and by using a locally

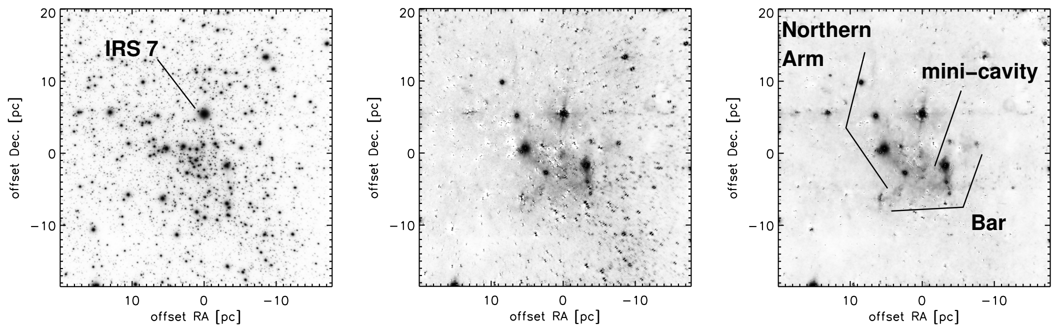

Figure 1: Images obtained along with all the procedure. *Left*: deep K_s-band mosaic centred on Sgr A*. *Middle*: the same image but with all the detected stars subtracted by using a single and constant PSF across the FOV. *Right*: Point source-subtracted K_s-band deep mosaic by using a local PSF kernel merged with a constant halo, determined from IRS 7. We can see the residuals due to consider the same PSF across the FOV. We use a logarithmic colour scale in all images. The middle and right panel have the same scale. North is up and East is to the left.

PSF kernel merged with a constant halo, respectively. We can see how we corrected the effect of the anisoplanatism that gives us an important source of residual in the image by using the variable core plus halo PSF.

3 Results

In order to study the existence of a relaxed cusp, we need to focus on stars that are at least several Gyr, similar to the relaxation time of the NSC at the GC (see [1]). The key point of our study is, on the one hand, pushing the completeness limit in stars counts about one magnitude deeper than in previous works and, on the other hand, study the surface brightness profile of the diffuse light, which traces even fainter stars. Figure 7 in [17] shows the K_s-Luminosity Function (KLF) determined from our deep mosaic. The new completeness limit from our work is $K_s \sim 18.5$, one magnitude deeper than in previous studies. Figure 16 of [30] shows the old star fraction, the mean stellar mass and the KLF as a function of theK_s magnitude based on a population synthesis model for the inner parsecs of the GC, assuming continuous star formation at a constant rate over the last 10 Gyr with a Miller-Scalo initial mass function [27]. We can see that the fraction of old stars reaches 80% at $K_s \sim 15.5$ magnitude, and again increases for $K_s > 17.5$. Whereas all the previous star density measurements were dominated by the RC and brighter giants ($K_s < 17.5$), now we can test two different new ranges of magnitude with a high fraction of old stars: faint stars with $17.5 \leq K_s \leq 18.5$ with masses of ~ 2.5 $M_\odot$ and even fainter, unresolved sources, with masses less than 1.5 $M_\odot$, probably sub-giants and MS stars.

The projected surface density of the old stars can be described by simple power laws

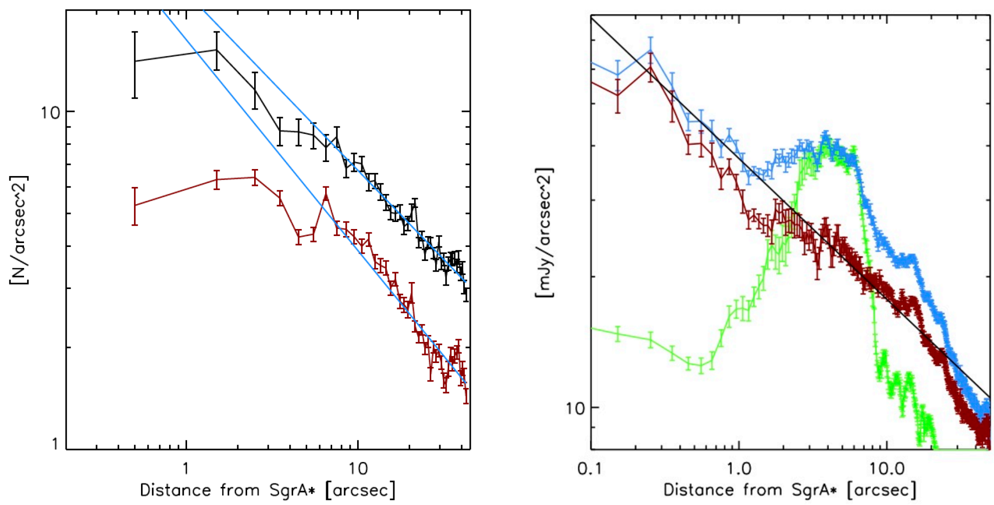

Figure 2: *Left*: Projected surface number density for giants (red) and faint stars (black). The blue lines are simple power-law fits to the data at 0.2 pc $\leq R \leq$ 1.0pc. *Right*: SB profile for the diffuse light for the wide-field K_s-image before (blue) and after (red) to the subtraction of the Paschen α emission (green). We multiply it by a adequate factor to optimise the plot. The black line is a simple power-law fit to the data at $R \leq 25''$(1 pc).

of the form $\Sigma(R) \propto R^{-\Gamma}$, where Σ is the surface number density, R the projected radius, and Γ the power-law index. We assume that the underlying spatial distribution of the stars in the central parsec is spherically symmetric, that is a good approximation for the central parsec. Table 2 in [17] show the different fits to the different distance ranges. The mean value and standard deviation for stars in the interval $17.5 \leq K_s \leq 18.5$ (faint stars) is $\Gamma_{faint} = 0.47 \pm 0.07$ (black line in right panel in Figure 2) and for stars in the magnitude interval $12.5 \leq K_s \leq 16$ (giants stars), $\Gamma_{giants} = 0.62 \pm 0.12$ (red line in right panel in Figure 2). For giants, only data at R $\geq 8''/0.24$pc gives us a good fit. The power law indices for the surface brightness (SB) profiles for the diffuse light are showns in Table 1 of [7]. The mean value is $\Gamma = 0.26 \pm 0.02_{stat} \pm 0.05_{sys}$.

To conclude, we aim to explore the 3D density structure of the stars near the massive black hole. Therefore, we need to convert the measure 2D profile into a 3D density law and deal with projection effects. For this reason, we have to add new data at projected radii R $\geq$ 2pc. We use the data from [16], that used extinction corrected near-infrared data from VLT/NACO, WFC/HST, and VISTA, and from [32], that used extinction-corrected Spitzer 4.5 μm. In order to isolate the star density of the NSC, we have to subtract from our sample the fore-/background contribution (NSD, GB, and GD). We used the Sérsic model for the non-NSC emission from Table 2 of [32]. Finally, in order to describe the 3D shape of the cluster, we use the *Nuker* model [23] as a generalization of a broken power law as given in equation 1 of [16]:

$$\rho(r) = \rho(r_b) 2^{(\beta-\gamma)/\alpha} \left(\frac{r}{r_b}\right)^{-\gamma} \left[1 + \left(\frac{r}{r_b}\right)^{\alpha}\right]^{(\gamma-\beta)/\alpha}, \tag{1}$$

where r is the 3D distance from the black hole, r_b is the break radius, ρ is the 3D density, γ is the exponent of the inner and β the one of the outer power-law, and α defines the sharpness of the transition. We projected it onto the sky via the following integral:

$$\rho(r) = \Sigma(R) = 2 \int_r^{\infty} \frac{r\rho(r)dr}{\sqrt{r^2 - R^2}}. \tag{2}$$

Table 4 from [17] and Table 2 from [33] show different Nuker fits for the data, exploring the effect of using different fore-/background emission models, fit ranges, integration boundaries and different values of the parameter α. We take the mean value of the best-fit parameters and the standard deviation. For the diffuse light we obtain: $r_b = 3.1 \pm 0.3$ pc, $\gamma = 1.13 \pm 0.03$, $\beta = 3.5 \pm 0.3$ and $\rho(r_b) = 0.028 \pm 0.005$ mJy arcsec^{-3}. For faint stars with $K_s \sim 18$, we consider explicitly the possible contamination by pre-MS stars in the star counts. We obtain a somehow larger value for the inner index $\gamma \approx 1.3$. For the RC and brighter giants, we have to exclude the inner data, obtaining a value of $\gamma \approx 1.53$. Like previous works, we do find a flat surface density inside around 0.3 pc of Sgr A*.

4 Discussion and conclusions

In order to clarify the controversial existence (or not) of the stellar cusp at the GC, we address the distribution of old stars around Sgr A* with improved methodologies. We push the completeness limit to reach the faintest stars studied so far and to test three different stellar populations, old enough to serve as tracers for the existence of a stellar cusp. We find that the stellar density decreases with a power-law index inside the range $\gamma = 1.1 - 1.4$ for distances smaller than the influence radius of Sgr A* (~ 3 pc). We can rule out a flat core with high confidence. The cusp is shallower than the predicted one by theory, but it can be explained if the star formation history of the NSC is taken into a count. In [5] a star cluster surrounding a central massive black hole is evolved over a Hubble time under the combined influence of two-body relaxation and continuous star formation. They compare their results with our observations, coming to an agreement between theory and observation for the first time. A caveat is a possible contamination by young stars in the distribution of faint stars. On the one hand, we explore explicitly the possible contamination by pre-MS stars, but on the other hand, we do not have data from stars that formed 100 Myr ago, although we know that the star formation rate in the central parsec was high in this epoch [29]. Like previous works, we find a lack of giants at projected distances of a few 0.1 pc of the supermassive black hole, that indicates some mechanism has altered their distribution. The number of missing giants estimated is on the order of 100.

Future works have to disentangle the intrinsic structure of the cusp, looking into the classification of the stars and rebuilding the 3D structure of the cluster by taking new faint and robust data to about 40 pc from the supermassive black hole. We are working on studing the different stellar populations across the NSC and improving the isolation of the NSC from the emission of the GB, GD, and NSD, taking into account more realistic models for them. The efforts made in clarifying our knowledge of the stellar cusp at the GC are fundamental for understanding not only the stellar dynamics at the GC but for the implications that have in other galactic nuclei and the observation of EMRIs with gravitational wave detectors in future observations.

Acknowledgments

The research leading to these results has received funding from the European Research Council under the European Union's Seventh Framework Programme (FP7/2007-2013) / ERC grant agreement n° [614922]. This work is based on observations made with ESO Telescopes at the La Silla Paranal Observatory under programmes IDs 183.B-0100 and 089.B-0162. We thank T. Fritz for detailed and valuable comments. This work has made use of the IAC-STAR Synthetic CMD computation code. IAC-STAR is suported and maintained by the computer division of the Instituto de Astrofísica de Canarias. PAS acknowledges support from the Ramón y Cajal Programme of the Ministry of Economy, Industry and Competitiveness of Spain. This work has been partially supported by the CAS President's International Fellowship Initiative.

References

[1] Alexander, T. 2005, physrep, 419, 65

[2] Amaro-Seoane, P., & Chen, X. 2014, apjl, 781, L18

[3] Bahcall, J. N., & Wolf, R. A. 1976, apj, 209, 214

[4] Bartko, H., Martins, F., Trippe, S., et al. 2010, apj, 708, 834

[5] Baumgardt, H., Amaro-Seoane, P., & Schödel, R. 2018, aap, 609, A28

[6] Boehle, A., Ghez, A. M., Schödel, R., et al. 2016, apj, 830, 17

[7] Buchholz, R. M., Schödel, R., & Eckart, A. 2009, aap, 499, 483

[8] Chatzopoulos, S., Fritz, T. K., Gerhard, O., et al. 2015, mnras, 447, 948

[9] Dale, J. E., Wünsch, R., Whitworth, A., & Palouš, J. 2009, mnras, 398, 1537

[10] Diolaiti, E., Bendinelli, O., Bonaccini, D., et al. 2000, aaps, 147, 335

[11] Do, T., Ghez, A. M., Morris, M. R., et al. 2009, apj, 703, 1323

[12] Dong, H., Wang, Q. D., Cotera, A., et al. 2011, mnras, 417, 114

[13] Feldmeier, A., Neumayer, N., Seth, A., et al. 2014, aap, 570, A2

[14] Feldmeier-Krause, A., Zhu, L., Neumayer, N., et al. 2017, mnras, 466, 4040

[15] Freitag, M., Amaro-Seoane, P., & Kalogera, V. 2006, apj, 649, 91

[16] Fritz, T. K., Chatzopoulos, S., Gerhard, O., et al. 2016, apj, 821, 44

[17] Gallego-Cano, E., Schödel, R., Dong, H., et al. 2018, aap, 609, A26

[18] Genzel, R., Eisenhauer, F., & Gillessen, S. 2010, Reviews of Modern Physics, 82, 3121

[19] Genzel, R., Schödel, R., Ott, T., et al. 2003, apj, 594, 812

[20] Gillessen, S., Plewa, P. M., Eisenhauer, F., et al. 2017, apj, 837, 30

[21] Gravity Collaboration, Abuter, R., Amorim, A., et al. 2018, aap, 615, L15

[22] Hopman, C., & Alexander, T. 2006, apjl, 645, L133

[23] Lauer, T. R., Ajhar, E. A., Byun, Y.-I., et al. 1995, aj, 110, 2622

[24] Lightman, A. P., & Shapiro, S. L. 1977, apj, 211, 244

[25] Merritt, D. 2010, apj, 718, 739

[26] Merritt, D., & Szell, A. 2006, apj, 648, 890

[27] Miller, G. E., & Scalo, J. M. 1979, apjs, 41, 513

[28] Neumayer, N. 2015, IAU General Assembly, 22, 2236674

[29] Pfuhl, O., Fritz, T. K., Zilka, M., et al. 2011, apj, 741, 108

[30] Schödel, R., Eckart, A., Alexander, T., et al. 2007, aap, 469, 125

[31] Schödel, R., Feldmeier, A., Kunneriath, D., et al. 2014, aap, 566, A47

[32] Schödel, R., Feldmeier, A., Neumayer, N., Meyer, L., & Yelda, S. 2014, Classical and Quantum Gravity, 31, 244007

[33] Schödel, R., Gallego-Cano, E., Dong, H., et al. 2018, aap, 609, A27

[34] Yusef-Zadeh, F., Bushouse, H., & Wardle, M. 2012, apj, 744, 24